A Conformational Change in Cytochrome *c* of Apoptotic and Necrotic Cells Is Detected by Monoclonal Antibody Binding and Mimicked by Association of the Native Antigen with Synthetic Phospholipid Vesicles†

Ronald Jemmerson,* Jiang Liu, Danielle Hausauer, Kong-Peng Lam,‡ Anna Mondino,§ and R. David Nelson

Department of Microbiology and Center for Immunology, University of Minnesota Medical School, Minneapolis, Minnesota 55455

Received April 23, 1998; Revised Manuscript Received January 20, 1999

ABSTRACT: By flow cytometry, a conformational change in mouse cytochrome *c* (cyt *c*) of apoptotic and necrotic T hybridoma cells was detected using a monoclonal antibody (mAb) that recognizes the region around amino acid residue 44 on a non-native form of the protein. The conformational change in cyt *c* is an early event in apoptosis, which can be identified in pre-apoptotic cells that are negative for other indicators of apoptosis. Since the mAb did not bind fixed and permeabilized live cells and did not immunoprecipitate soluble cyt *c* extracted with detergent from dead cells, it appears to recognize cyt *c* bound in a detergent-sensitive complex to other cellular components. Coincidentally, the mAb was also shown by competitive enzyme-linked immunosorbent assay to bind cyt *c* associated with synthetic phosphatidic acid vesicles. This suggests that the conformational change of cyt *c* in dying cells could be due to its association with intracellular membranes that are, perhaps, altered in cell death. By immunofluorescent confocal microscopy, conformationally altered cyt *c* in post-apoptotic T hybridoma cells showed a punctate distribution, indicating that it remained associated with mitochondria. Furthermore, the heavy membrane fraction of post-apoptotic cells but not of live cells was functional in caspase activation. This suggests that membrane-bound cyt *c* is the relevant caspase coactivation factor in the T hybridoma cells.

Employing biophysical methods, e.g., resonance Raman spectroscopy (*1*), ^{1}H, ^{13}C, and ^{31}P nuclear magnetic resonance (*2*−*5*), Fourier transform infrared spectroscopy (*6*), and differential scanning calorimetry (*6*), a number of investigators have demonstrated a conformational change in cyt *c*[1] when the protein associates with synthetic anionic phospholipid vesicles. The conformational change involves an opening of the heme crevice resulting, in part, from the loss of both the iron−methionine 80 ligation (*3*) and H-bonds between amino acid side chains and one of the heme propionates (*5*), as well as destabilization of the tertiary structure of the polypeptide detected by the accessibility of the backbone amides to hydrogen−deuterium exchange (*6*). It has not been conclusively determined whether this conformational change has any biological significance. Although cyt *c*−phospholipid interactions are considered to be a paradigm for the putative interaction of cyt *c* with the phospholipid-rich inner mitochondrial membrane (*7*), support for it from in situ analysis of cyt *c* in intact cells is lacking.

mAbs are sensitive to the conformation of a protein antigen (*8*, *9*). Thus, they can be useful tools for localizing conformational changes in a polypeptide and for tracking conformational changes that may occur in proteins in situ. Over the years, we have obtained a number of mAbs specific for native and non-native forms of cyt *c* (*10*−*12*). These mAbs have not previously been examined for their ability to recognize cyt *c* within cells. Here we report the results of such a study in which flow cytometry (FACS) and confocal microscopy were employed to examine the binding of mAbs to cyt *c* in a T cell hybridoma, DO11.10 (*13*). Since cyt *c* has recently been reported to translocate early in cell death from its normal location in the space between the inner and outer mitochondrial membranes (*14*), we have examined mAb binding to cyt *c* in apoptotic and necrotic cells as well as in live cells.

The results show that cyt *c* undergoes a conformational change early in apoptosis and in necrosis. The mAb detecting this change recognizes the omega loop region around residue 44, which is located to the right of and below the exposed heme crevice (*15*), on a native-like form of cyt *c*. Although this mAb binds neither purified native cyt *c* nor cyt *c* in permeabilized live cells, it does recognize cyt *c* in association with synthetic phospholipid vesicles. Failure of the mAb to

† Supported by Grant MCB-9630412 from the National Science Foundation.

* To whom correspondence should be addressed: Department of Microbiology, University of Minnesota Medical School, Box 196 FUMC, 420 Delaware St. S.E., Minneapolis, MN 55455.

‡ Present address: Institute of Genetics, University of Koln, D-50931 Cologne, Germany.

§ Present address: Unita' di Genetica Molecolare, DIBIT, H. S. R., Milano 20132, Italy.

[1] Abbreviations: Apaf, apoptotic protease activating factor; 7-AAD, 7-aminoactinomycin D; CNBr, cyanogen bromide; cyt *c*, cytochrome *c*; ELISA, enzyme-linked immunosorbent assay; FACS, fluorescence-activated cell scanning; FI, fluorescence intensity; FITC, fluorescein isothiocyanate; FSC, forward scatter; mAb, monoclonal antibody; OVA, ovalbumin; PA, phosphatidic acid; PARP, poly(ADP-ribose) polymerase; SSC, side scatter.

10.1021/bi9809268 CCC: $18.00
Published on Web 02/27/1999

Table 1: Cyt *c*-Specific mAbs Employed in This Study

mAb	immunogen	reactivity[a]	isotype	ref
2.7D5	pigeon cyt *c*−OVA	residue 62 of native mouse cyt *c*	IgG2a,κ	*b*
1E8	rat cyt *c*−OVA	residue 62 of native mouse cyt *c*	IgG1,κ	*11*
2G8.B6	rat cyt *c*−OVA	residue 62 of native mouse cyt *c*	IgG1,κ	*12*
2G8.B9	rat cyt *c*−OVA	residue 44 of native mouse cyt *c*	IgG2a,κ	*28*
1D3	cow cyt *c*−OVA	residue 44 of non-native mouse cyt *c*	IgG1,κ	*29*
7H8	horse cyt *c*−OVA	residues 93−104 of non-native mouse cyt *c*	IgG2b,κ	*23*

[a] Except for mAb 7H8, only the dominant amino acid residue affecting the binding of the mAbs is given. The actual binding sites encompass larger regions around the indicated residue. The mAbs may react with some other cyts *c*, e.g., the immunizing cyts *c*. [b] R. Jemmerson, R. D. Nelson, C. M. Mueller, and J. M. Minnerath, manuscript in preparation.

immunoprecipitate cyt *c* from apoptotic and necrotic cells indicates that the conformational alteration in cyt *c* that is detected by this mAb is not due to a covalent modification and is consistent with a membrane association-induced conformational change.

This study introduces potential physiological significance to the altered conformation of cyt *c* shown previously to occur when the protein associates with synthetic phospholipid vesicles. However, contrary to the current paradigm, the conformational change in cyt *c*, at least that which is detected by the mAb in this study, does not occur as cyt *c* associates with the inner mitochondrial membrane components in their normal array since the mAb does not recognize cyt *c* in permeabilized, live cells. The conformationally altered membrane-bound form of cyt *c* appears to be relevant to its role in apoptotic cell death in the T hybridoma cells studied since the heavy membrane fraction containing mitochondria retained the potential for caspase coactivation in the presence of normal cytosolic components. Since cyt *c* is a self-antigen and is known to elicit antibodies in some cases of autoimmunity (*16*), the conformational change in cyt *c* described here may have implications in the recognition of "self" cyt *c* by B lymphocytes.

MATERIALS AND METHODS

Cells. The mouse T cell hybridoma, DO11.10 (*13*), was obtained from M. Jenkins (University of Minnesota). Cells were cultured in Dulbecco's modified Eagle's medium containing sodium pyruvate, glutamine, 15% fetal bovine serum, and penicillin/streptomycin in an atmosphere of 5% CO_2 and air.

Antigens and Antibodies. Rat, rabbit, and horse cyts *c* were obtained from Sigma Chemical Co. (St. Louis, MO) and purified by ion-exchange chromatography on carboxymethyl-Sephadex in 65 mM sodium phosphate (pH 7.5). Since mouse and rat cyts *c* are identical (*17*), herein rat cyt *c* will be referred to as mouse cyt *c*. Cow, dog, donkey, and guanaco cyts *c* were provided by E. Margoliash (The University of Illinois at Chicago, Chicago, IL). The 1−80 and 1−65 (residues) heme-containing fragments of horse cyt *c* were prepared by CNBr cleavage and purified by gel filtration chromatography on Sephadex G-50 in 7% formic acid (*18*). The N-acetylated 1−4, 93−104, 41−48, and 40−54 (residues) peptides of horse cyt *c* were synthesized by solid-phase methods, purified by reverse-phase high-performance liquid chromatography using a C18 column and a linear gradient of 0 to 60% acetonitrile, and characterized as previously described (*19*). Most of the mAbs in this study have been described previously (see Table 1). Polyclonal antibodies to the 1−80 fragment were obtained by immunizing mice with the fragment coupled to hemocyanin using glutaraldehyde. BALB/c mice (strain AnNCrlBr, Charles River Breeding Laboratories, Wilmington, MA) were injected intraperitoneally with 50 μg of the complex emulsified 1:1 in complete Freund's adjuvant. Four weeks later, the mice were similarly challenged and antibodies were obtained from ascites fluid that spontaneously developed in the mice. Polyclonal antibodies and mAbs were purified by adsorption on the appropriate antigen-coupled CNBr-activated Sepharose 4B (Sigma Chemical Co.; *20*). mAbs 2.7D5, 2G8.B9, 1E8, and 2G8.B6 were adsorbed on rat cyt *c*−Sepharose and mAb 1D3, anti-1−4, anti-41−48, and anti-1−80 polyclonal antibodies on horse cyt *c*−1−80-Sepharose; mAb 7H8 was adsorbed on 93−104-Sepharose. The antibodies were eluted in 0.5 M acetic acid, neutralized with a half-volume of 2 M Tris, and dialyzed against 2 × 3 L of phosphate-buffered saline for 48 h. Following this treatment, the antibodies retained their ability to bind their respective antigens in ELISAs.

ELISA. Specificities of the mAbs were previously determined (*10*−*12*). In this study, mAb 1D3 was further characterized by indirect and competitive ELISAs, both previously described (*21*). For indirect ELISAs, various cyts *c* (0.5 μM) in phosphate-buffered saline (pH 7.4) were adsorbed to Nunc Maxisorp microtiter plates (Gibco, Coon Rapids, MN). Binding of mAb 1D3 to antigen on the plates was detected using horseradish peroxidase conjugated to goat anti-mouse IgG (whole molecule; Pierce Chemical Co., Rockford, IL) and *o*-phenylenediamine as chromogen in the catalysis of hydrogen peroxide. For competitive ELISAs, cyt *c* was bound to microtiter plates and various soluble antigens (100 μM to 1 nM) diluted in 5% horse serum, or cyt *c*-associated phospholipid vesicles (see below) also diluted in 5% horse serum were examined for their ability to block the binding of mAb 1D3 to plate-bound cyt *c*. In this assay, mAb 1D3 was diluted such that its binding to cyt *c* in an indirect ELISA was approximately half-maximal.

Preparation of Synthetic Phospholipid Vesicles. L-α-PA (Sigma Chemical Co.) was dissolved in chloroform and ethanol (1:1) to a concentration of 10 mM and stored at −20 °C. For vesicle preparation (*22*), the dissolved PA was dried under a stream of N_2 and maintained under vacuum for at least 2 h. It was hydrated in 20 mM Hepes and 0.1 mM EDTA (pH 6.8) and vortexed for l min to obtain unilamellar vesicles. Cyt *c* (720 μg) was mixed with 50 μL of vesicles (20 mM PA) and incubated at room temperature for 1.5 h.

Cross-Linking Cyt c and OVA. Mouse cyt *c* (1 mg) was coupled to OVA (1 mg) using glutaraldehyde (0.1%) in 65 mM phosphate (pH 7.5) or in 0.1 M sodium carbonate (pH

9.8). Cyt *c*−OVA complexes were dialyzed twice against 3 L of phosphate-buffered saline (pH 7.4).

Immunoprecipitation of Cyt c Extracted from DO11.10 Cells and Western Blot Analysis. Cells were suspended at a density of 10^8 per mL in lysis buffer containing 1% NP-40, 50 mM Tris-HCl (pH 8.0), 150 mM sodium chloride, 0.02% sodium azide, 100 μg/mL phenylmethanesulfonyl fluoride, and protease inhibitor cocktail (Boehringer Mannheim, Indianapolis, IN). The cells were incubated on ice for 20 min and centrifuged at 10 000 rpm for 5 min at 4 °C in a microfuge. The supernatant (0.1 mL) was incubated with 15 μg of mAb and 15 μL of a protein G−agarose slurry (ImmunoPure, Pierce Chemical Co.). After overnight incubation with mixing at 4 °C, the protein G−agarose was washed three times with 0.5 mL of lysis buffer, then resuspended in 30 μL of SDS−PAGE loading buffer containing 2-mercaptoethanol, and boiled for 3 min. Following centrifugation, the supernatants were loaded onto a 15% polyacrylamide gel and electrophoresed. The proteins were electroblotted onto a nitrocellulose membrane and probed with mAb 7H8 that was reactive with the carboxyl terminus of cyt *c* (*14*, *23*). Binding by the mAb was visualized using horseradish peroxidase-conjugated goat anti-mouse IgG and Amersham's ECL kit (Arlington Heights, IL).

Induction of Apoptosis and Necrosis. Generally, DO11.10 cells were treated with dexamethasone (4 μg/mL) for 18 h to induce apoptosis (*24*). In some experiments, the cells received 3000 R γ-irradiation (cesium source) or were incubated overnight in 24-well plates coated with an anti-CD3 mAb (145-2C11 from PharMingen, San Diego, CA; *25*). To mimic necrosis, cells were heated to 65 °C in a water bath for 5 min.

Immunofluorescent Labeling and Flow Cytometry. DO11.10 cells (1×10^6) were indirectly labeled at 4 °C using 0.1−5 μg of anti-cyt *c* mAbs or polyclonal antibodies in 0.2 mL of labeling buffer [phosphate-buffered saline (pH 7.4) containing 2% fetal bovine serum and 0.2% sodium azide] followed 30 min later, after several washes in labeling buffer, by FITC-conjugated goat anti-mouse IgG or FITC-conjugated anti-rabbit IgG antibodies (both γ-chain specific and diluted 1:300; Sigma Chemical Co.). Cells were washed twice in labeling buffer and then analyzed. Control antibodies included mouse IgG1, IgG2a, and IgG2b mAbs (Caltag Labs, South San Francisco, CA), an IgG2a mAb (B10) specific for human placental alkaline phosphatase (*26*), and normal rabbit IgG from serum. In some cases prior to labeling, cells were fixed in 2% paraformaldehyde at room temperature for 20 min and then permeabilized in labeling buffer containing 0.5% Triton X-100; in all subsequent steps, the detergent-containing labeling buffer was used. Immunofluorescence was detected by flow cytometry employing a FACScan apparatus (Becton-Dickinson, San Jose, CA). Generally, 20 000 cells were analyzed for each labeling condition. After data collection, gates were selected on the basis of the FSC versus SSC. Live, apoptotic, and necrotic cells were distinguished by these criteria and also by differential uptake of 7-AAD (Calbiochem, La Jolla, CA), 2 μL of which was added at the end of the immunofluorescent labeling procedure to cells suspended in 0.1 mL of phosphate-buffered saline, or by staining with FITC-annexin V (annexin-V-FLUOS staining kit, Boehringer Mannheim).

Confocal Microscopy. DO11.10 cells were immunofluorescently labeled as they were for flow cytometry, fixed in 4% paraformaldehyde for 30 min at room temperature, and dried onto glass slides. Control mAbs included B10 (IgG2a) and a mAb against toxic shock syndrome toxin-1 (IgG1; provided by P. Schlievert, University of Minnesota). The cells were covered with Permount (Fisher Scientific, Chicago, IL) containing 50−100 μm glass beads (Polysciences, Inc., Warrington, PA) and then sealed under a coverslip. Confocal microscopy was performed as described previously (*27*). Images were collected using a Bio-Rad Laser Sharp 1024 confocal microscope (Bio-Rad, Hercules, CA). Digitized images were converted to photomicrographs (Confocal Assistant, Minneapolis, MN).

Extraction of Mitochondria and Assay for Caspase Activation. Live and dexamethasone-treated DO11 cells (5×10^7) were lysed on ice for 10 min in 10 mM Hepes buffer (pH 7.0) containing 0.5 mM $MgCl_2$, 1 mM dithiothreitol, 250 mM sucrose, 0.1 mM phenylmethanesulfonyl fluoride, 5 μg/mL pepstatin, 10 μg/mL leupeptin, and 2 μg/mL aprotinin. These conditions are a modification of the standard fractionation buffer (lower pH and lower ionic strength) so any membrane-bound cyt *c* could be encouraged to remain associated with membranes. The cells were homogenized in a scintered glass douncer, microfuged to pellet nuclei, and centrifuged at 100000*g* to obtain the heavy membrane (mitochondria-containing) fraction and S-100 supernatant. The membrane fraction was washed three times in 30 volumes each of lysis buffer. Prior to the assay for caspase coactivation, the cell fractions were modified to achieve the standard conditions for the assay, i.e., 25 mM Hepes (pH 7.5), 10 mM KCl, 1.5 mM $MgCl_2$, 1 mM sodium EDTA, 1 mM EGTA, 1 mM dithiothreitol, 250 mM sucrose, and protease inhibitors as described above. To assay for PARP cleavage, S-100 and heavy membrane fractions (up to 10 μL or ~25% of the total membranes) from live and apoptotic cells were added to the S-100 fraction of live cells along with dATP to a final concentration of 2 mM and 150 ng of PARP (Biomol Research Laboratories, Plymouth Meeting, PA). The mixtures were incubated at 37 °C for 1 h. Intact PARP and its cleavage products were resolved by SDS−PAGE in an 8% gel, electrophoretically transferred to a nitrocellulose membrane, and probed using anti-PARP mAb C-2-10 (Biomol Research Laboratories). PARP-related bands were visualized in the Western blot using horseradish peroxidase coupled to goat anti-mouse IgG and enhanced chemiluminescence (ECL) detection reagents (Amersham Life Science, Arlington Heights, IL).

RESULTS

Antibodies That Are Reactive with Native and Non-Native Forms of Cyt c. In this study, we attempted to detect cyt *c* in live, apoptotic, and necrotic cells by indirect immunofluorescence using a panel of mAbs listed in Table 1 as well as with several polyclonal peptide-reactive antibodies. mAbs reactive to the two defined antigenic regions of native cyt *c*, around residues 44 and 62, were used to detect the native form. mAbs 2.7D5, 1E8, and 2G8.B6 recognize the region around residue 62 on native mouse cyt *c* (*11*, *12*; unpublished results). Since mAb 2.7D5 was elicited against pigeon cyt *c* coupled to OVA, it has some differences in specificity from the other two mAbs which were elicited against mouse cyt

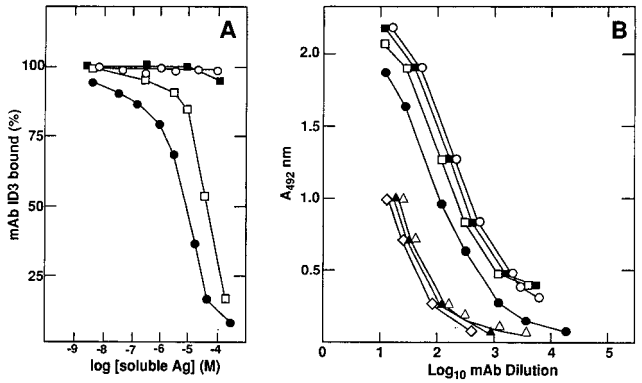

FIGURE 1: mAb 1D3 is specific for a non-native form of cyt *c* and binds in the region around residue 44. (A) Binding of mAb 1D3 to cow cyt *c* adsorbed to microtiter plates was inhibited in a competitive ELISA by soluble cyt *c* fragment 1−80 (●) and 1−65 (□), but not by native horse cyt *c* (○). The synthetic 40−54 peptide (■) slightly inhibited binding at higher concentrations. (B) Binding of mAb 1D3 (~4 μg/mL undiluted) to various cyts *c* in an indirect ELISA shows sensitivity of the mAb to amino acid residue changes at position 44: horse (●), cow (○), dog (■), donkey (□), rabbit (△), guanaco (▲), and mouse (◇). Mouse cyt *c* has alanine at position 44; rabbit and guanaco cyts *c* have valine, and the other cyts *c* listed have proline.

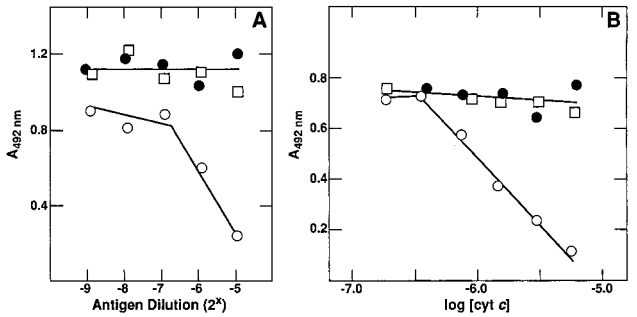

FIGURE 2: mAb 1D3 recognizes a conformational change in cyt *c* that occurs when the protein associates with phospholipid vesicles (A) or when cyt *c* is cross-linked to OVA at alkaline pH (B). In a competitive ELISA with rabbit cyt *c* adsorbed to a microtiter plate (A), rabbit cyt *c* bound to PA-containing phospholipid vesicles (○), PA-containing phospholipid vesicles alone (●), and soluble rabbit cyt *c* (□) were examined for their ability to inhibit the binding of mAb 1D3 to cyt *c* on the assay plate. The undiluted concentration of rabbit cyt *c* was 2 mM and that of PA 20 mM. In a similar assay with rat cyt *c* adsorbed to a microtiter plate (B), rat cyt *c*−OVA coupled at pH 9.8 (○), rat cyt *c*−OVA coupled at pH 7.5 (●), and rat cyt *c* alone (□) were examined for their ability to inhibit the binding of mAb 1D3 to rat cyt *c* adsorbed to a microtiter plate.

c coupled to OVA. mAb 2G8.B9 recognizes the region on native mouse cyt *c* around residue 44 (*28*).

Two mAbs which were elicited in the antibody response to intact cyt *c* but which react with peptides other than the native protein were used to try to detect non-native cyt *c* in the cells. mAb 7H8 recognizes the carboxyl terminal peptide of residues 93−104 (*23*). mAb 1D3 reacts with peptides containing the amino acids 40−54 of cyt *c*. This mAb was partially described previously (*29*). As shown in Figure 1A, in a competitive ELISA with the immunogen for 1D3 (cow cyt *c*) adsorbed to microtiter wells, native horse cyt *c* failed to block the binding of mAb 1D3. Similar results were observed using mouse cyt *c* even when as much as 200 μmol of soluble antigen was used (not shown). Slight but reproducible inhibition was observed by the soluble 40−54 peptide when mAb 1D3 was tested using the 1−80 peptide fragment adsorbed to microtiter wells (Figure 1A). The longer 1−65 peptide fragment was a more effective inhibitor of mAb 1D3 than the shorter peptide, and the 1−80 fragment was the most effective inhibitor of the peptides examined. In previously published data from an experiment with the weaker binding 1−65 fragment of horse cyt *c* adsorbed to microtiter wells, the 40−54 peptide did show significant inhibition (>60% at 100 μM peptide) while the 41−48 peptide and native horse cyt *c* did not inhibit (*29*).

Although mAb 1D3 does not bind native cyt *c*, it recognizes a conformation of the protein obtained when some molecules adsorb to microtiter wells in ELISA. By comparison of the binding of mAb 1D3 to different cyts *c* in an indirect ELISA, it was apparent that residue 44 was involved in the recognition. Thus, cyts *c* with proline at position 44 (horse, cow, dog, and donkey) generally bound more effectively than cyts *c* with valine (rabbit and guanaco cyts *c*) or alanine (mouse cyt *c*) at position 44 (Figure 1B). The slightly decreased level of binding of mAb 1D3 to horse cyt *c* compared to those of the other cyts *c* with proline at position 44 is likely due to a threonine residue at position 47 in horse cyt *c*, whereas the other cyts *c* tested have serine at that position (*17*).

mAb 1D3 Recognizes Cyt c Associated with Synthetic Phospholipid Vesicles. It has been reported that association of cyt *c* with synthetic phospholipid vesicles causes a conformational change with the loss of the methionine 80−heme iron ligand (*3*) and H-bonds between one of the heme propionates and amino acid residues 39, 49, 78, and/or 79 (*5*), leading to the opening of the heme crevice. Since mAb 1D3 recognizes on non-native cyt *c* a region containing the omega loop around residue 44 which is situated to the right and below the heme crevice (*15*), it seemed possible that this mAb might recognize the conformational change that occurs in cyt *c* as it associates with synthetic phospholipid vesicles. To examine this possibility, synthetic liposomes were prepared from PA and then incubated with native cyt *c*. PA was chosen since cyt *c* has been reported to have the highest affinity for this phospholipid (*30*). The cyt *c*-associated vesicles were examined by a competitive ELISA for their ability to inhibit the binding of mAb 1D3 to cyt *c* attached to microtiter plates. The results shown in Figure 2A indicate that mAb 1D3 does recognize cyt *c* in association with synthetic phospholipid vesicles. Only when the native cyt *c* was preincubated with the vesicles was it able to inhibit the binding of mAb 1D3 to cyt *c* on the microtiter plate. Neither free native cyt *c* nor the phospholipid vesicles themselves inhibited the binding of mAb 1D3 to plate-bound cyt *c* in a competitive ELISA (Figure 2A).

The conformational change that occurs in cyt *c* when it is bound to negatively charged phospholipids appears to be similar to the change that occurs in cyt *c* when the pH is elevated above 9.35 (*31*). Therefore, we investigated the binding of mAb 1D3 to the alkaline isomer of cyt *c*. Since pH could affect mAb binding, we attempted to fix the alkaline conformation in cyt *c* by cross-linking it to OVA at pH 9.8 using glutaraldehyde. The "alkaline" cyt *c*−OVA complex was then brought to neutral pH by dialysis. By a competitive ELISA (Figure 2B), it was shown that mAb 1D3 does recognize the alkaline isomer of cyt *c*. Thus, mouse cyt *c* cross-linked to OVA at pH 9.8 did inhibit the binding of mAb 1D3 to mouse cyt *c* adsorbed to microtiter plates,

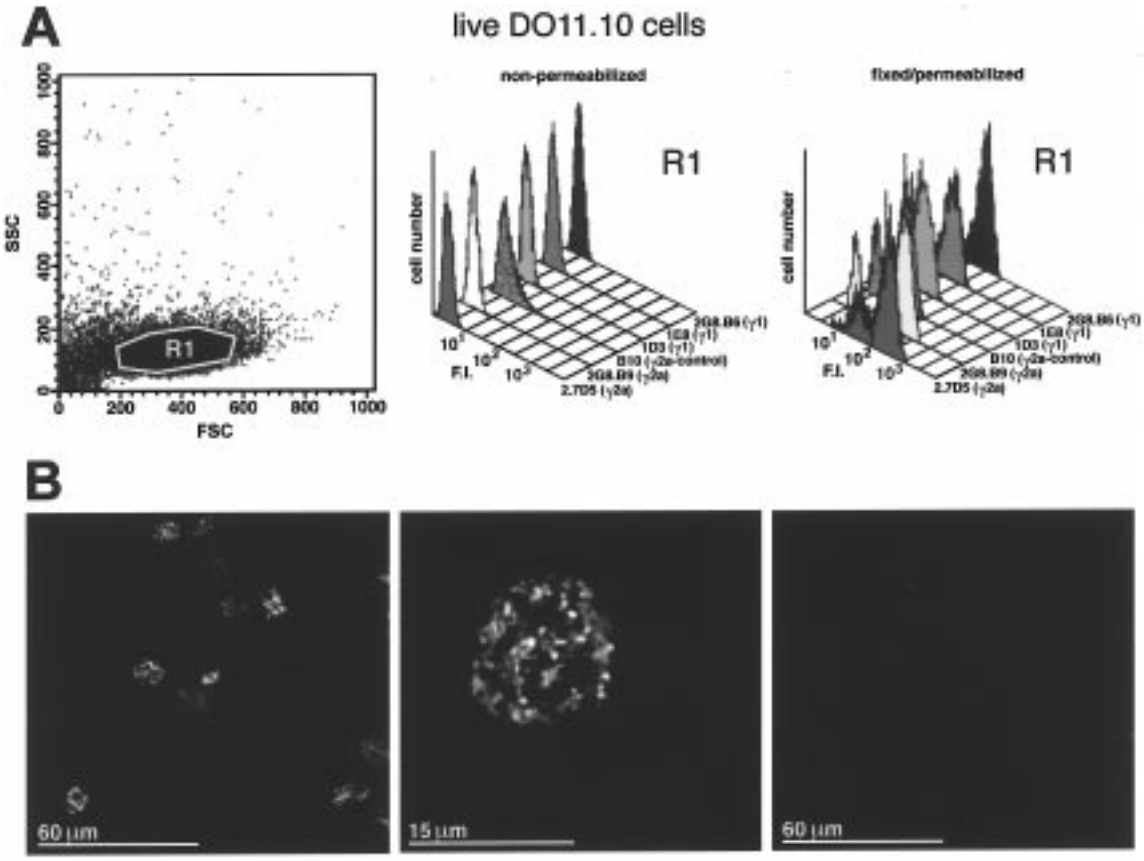

FIGURE 3: Indirect immunofluorescent labeling of intracellular mouse cyt *c* in live DO11.10 T hybridoma cells visualized by (A) flow cytometry and (B) confocal microscopy. Recognition of cyt *c* by mAbs required detergent permeabilization of the cells. Cells were incubated with 5 μg of each mAb followed by FITC-goat anti-mouse IgG. (A) FI (middle and right panels) is shown for cells within the R1 gated population (left panel). The same background level of fluorescence observed with IgG1 mAbs 1D3, 1E8, and 2G8.B6 (mean FI of 14−22 for permeabilized cells) was observed when cells were incubated with 0.1 μg of control IgG1 mAb (not shown). In live cells, the level of binding by mAb 2G8.B9 was much greater than that for the control IgG2a mAb (B10) (a mean FI of 192 compared to a mean FI of 41). (B) The fluorescence resulting from mAb 2.7D5 labeling of several DO11.10 cells (left panel) and of a single cell at a greater magnification (middle panel) is projected as a three-dimensional image; i.e., fluorescence throughout the cell is observed, not just the fluorescence in an optical section as appears in Figure 5. No labeling was observed with the isotype-matched control mAb B10 (right panel) (magnification, 100× objective; left panel = 1 zoom, middle panel = 4 zoom, and right panel = 1 zoom).

whereas mouse cyt *c* cross-linked to OVA at pH 7.5 did not inhibit the binding of mAb 1D3.

Detection of Cyt c in Viable Cells. Immunofluorescent labeling of cyt *c* in mouse hybridoma DO11.10 cells was analyzed by flow cytometry. Results of the labeling of live cells are shown in Figure 3A. Gates were set on the R1 (viable) population to eliminate any dead cells present [near the origin in the FSC (size) vs SSC (granularity) plot]. None of the anti-cyt *c* mAbs labeled cyt *c* in viable cells unless the cells were fixed and permeabilized. This is as expected since native cyt *c* is present in mitochondria of live cells and would not be accessible for antibody recognition without permeabilizing the cell and organelle membranes. However, not all of the mAbs labeled cyt *c* in the permeabilized cells. Only one of the mAbs (2.7D5) recognizing the surface around residue 62 bound cyt *c* in the cells. The other two mAbs, 1E8 and 2G8.B6, did not, even though all three mAbs immunoprecipitated cyt *c* that was extracted from live cells in detergent (results not shown). In these experiments, 5 μg of each mAb was used to label 10^6 cells, although the maximum specific fluorescence for mAb 2.7D5 was attained at 1 μg (results not shown). Compared to untreated cells, there was increased fluorescence in the fixed and permeabilized cells for each mAb tested. However, this was nonspecific since it was also observed in cells incubated with the control mAbs. The same mean fluorescence was observed with the control IgG1,κ mAb (0.1 μg; results not shown) and cyt *c*-specific mAbs 1E8 and 2G8.B6 (5 μg). The region around residue 44 was detected on native mouse cyt *c* in the live cells by mAb 2G8.B9. None of the antibodies that were reactive with short or long peptides of cyt *c* labeled fixed and permeabilized live cells (e.g., mAb 1D3 in Figure 3A and results not shown). In confocal microscopy, the anti-native cyt *c* mAbs labeled the cells intracellularly in a punctate fashion as would be expected of a mAb binding a mitochondrial protein. Results using mAb 2.7D5 are shown in Figure 3B (left and middle panels). The isotype-matched control mAb B10 did not label the fixed, permeabilized cells (Figure 3B, right panel).

Detection of Cyt c in Apoptotic Cells. For most experiments, apoptosis was induced in the DO11.10 T hybridoma cells using dexamethasone as described previously (*24*). This treatment affected the uptake of 7-AAD and staining with FITC-annexin V, both markers for apoptosis as will be discussed below, and altered the FSC versus SSC profile of the cells (Figure 4A). DO11.10 cells designated R2 are smaller and slightly more granular than live cells. Since cells in the R2 subpopulation have lost their membrane integrity (see below), they will be referred to hereon as post-apoptotic. Cells in another subpopulation of dexamethasone-treated

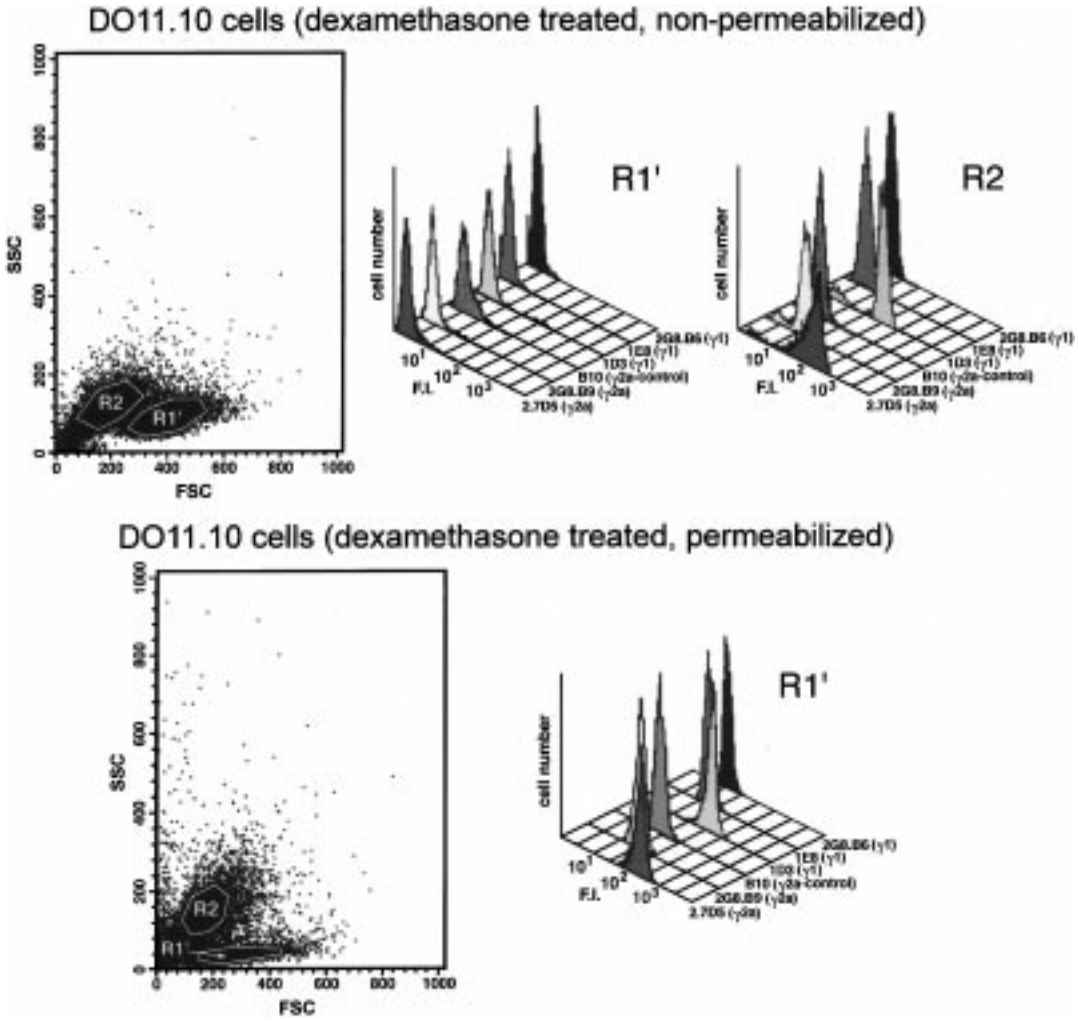

FIGURE 4: Immunofluorescent labeling of cyt *c* in apoptotic DO11.10 cells visualized by flow cytometry. Gates were set for the two subpopulations in the apoptotic cells based on the FSC vs SSC (left panels). In nonpermeabilized cells (top panel), only the R2 subpopulation was labeled by the cyt *c*-specific mAbs. Binding by mAb 1D3 and a decreased level of binding by mAb 2G8.B9 (relative to the level of binding observed in live cells in Figure 3) indicate a conformational change in the region around residue 44 on cyt *c*. In the top right panel, the mean FI of 17 for mAb 2G8.B9 is compared to the mean FI of 8 for the control mAb B10. Thus, there is significant binding, albeit at a reduced level, by the cyt *c*-specific mAb 2G8.B9 which may not be apparent in the figure. In the bottom panel, permeabilized R1′ cells show a pattern of specific mAb labeling similar to that seen in the nonpermeabilized R2 subpopulation.

DO11.10 cells (designated R1′) are larger than cells in the R2 population and no more granular than live cells (compare Figures 3A and 4A). Since R1′ and R2 differ in FSC versus SSC, in their uptake of 7-AAD, and in their staining with FITC-annexin V (see below), they appear to be at different stages of apoptosis.

Cyt *c* was detected by mAb binding in the R2 post-apoptotic population of DO11.10 cells without fixation and/or permeabilization. While mAbs to both the regions around residue 44 and residue 62 bound cyt *c* of post-apoptotic DO11.10 cells, the level of binding by mAb 2G8.B9 was significantly reduced (>90%) relative to its level of binding to cyt *c* in live cells. However, binding by mAb 1D3 which was not observed in the fixed and/or permeabilized live cells was now apparent (Figure 4, top right). Cyt *c*-specific mAb labeling of the R1′ subpopulation of DO11.10 cells was only observed following fixation and/or permeabilization (Figure 4, bottom), and then the level of relative labeling by the mAbs was similar to the level of surface labeling of the R2 subpopulation. This is consistent with the R1′ subpopulation being at an early stage of apoptosis.

When visualized by confocal microscopy, indirect immunofluorescent staining of cyt *c* in post-apoptotic cells showed a different pattern than was observed when cyt *c* was immunolabeled in live cells. Shown in Figure 5 are optical sections through a post-apoptotic DO11.10 cell indirectly labeled with mAb 2.7D5 (top, left panel) and 1D3 (bottom, left panel). Much of the staining is punctate, distributed more toward the surface than was observed in live cells. What would appear to be surface-displaced mitochondria are reminiscent of small blebs containing components of the endoplasmic reticulum, ribosomes, and nucleus that previously have been observed in apoptotic cells (*32*). In addition to the punctate mAb staining, some staining appears to be more diffuse but in patches toward one pole in the middle of the cell, possibly aggregates of partially degraded mitochondria.

Detection of Cyt c in Necrotic Cells. To mimic necrosis, cells were heat shocked for 5 min at 65 °C. Following this treatment, a single population of cells (designated R3) was observed on the basis of FSC versus SSC (Figure 6). Cells in the R3 population of DO11.10 cells were more granular

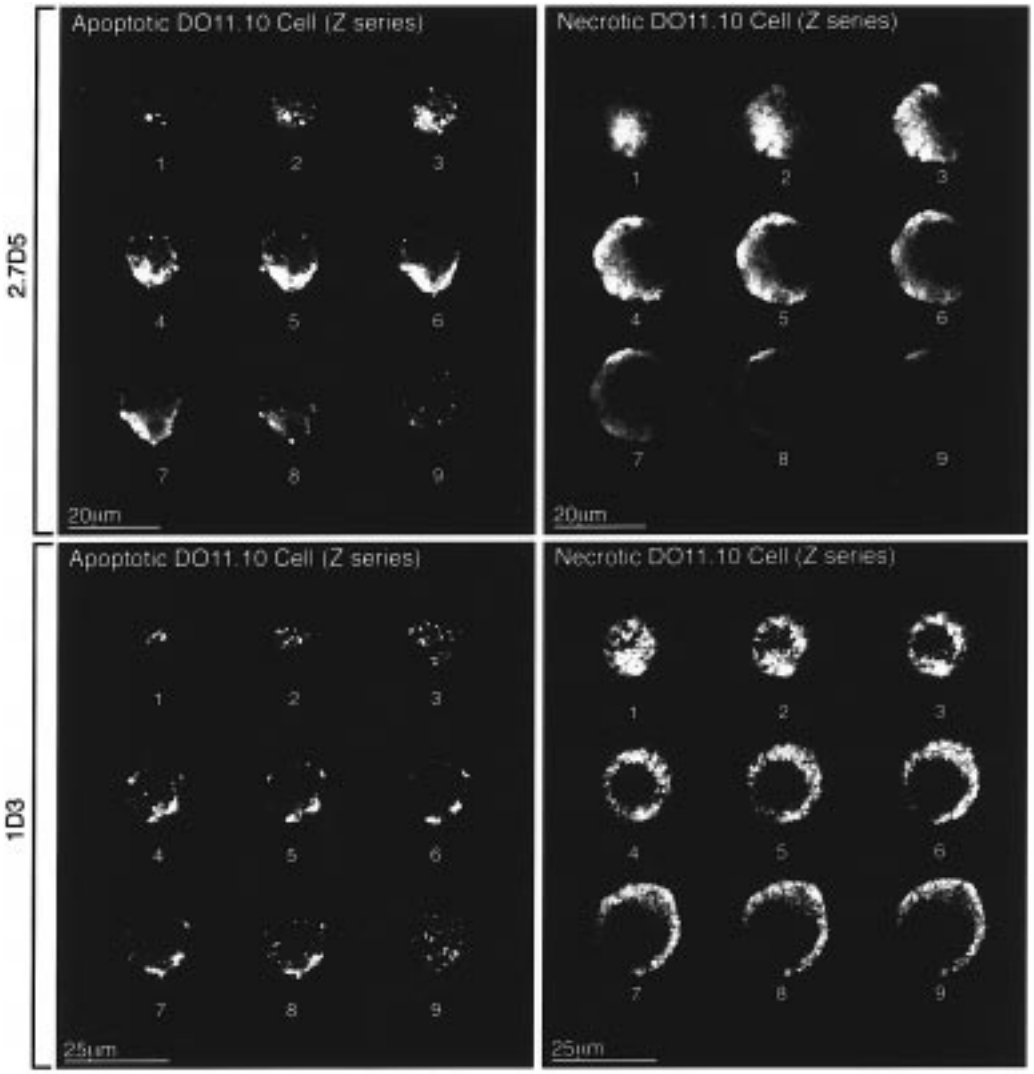

FIGURE 5: Confocal immunofluorescent microscopy of apoptotic (left panel) and necrotic (right panel) DO11.10 cells indirectly labeled with cyt *c*-specific mAbs 2.7D5 or 1D3 and FITC-goat anti-mouse IgG. Fluorescence is shown in equally spaced optical sections (Z series 0.5 μm steps) through individual cells. No labeling was apparent when the control mAb IgG1 and IgG2a mAbs were examined (results not shown) (magnification, 100× objective; 4 zoom)

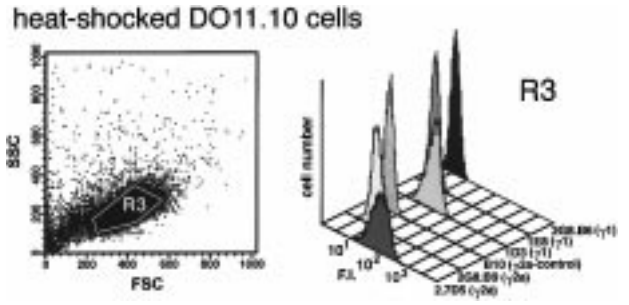

FIGURE 6: Indirect immunofluorescent labeling of cyt *c* in necrotic DO11.10 cells visualized by flow cytometry. Cells were heat shocked at 65 °C for 5 min prior to labeling. Cyt *c* undergoes the same conformational change in necrotic cells shown by the level of binding of mAb 1D3 relative to that of mAb 2G8.B9 as occurs in apoptotic cells. mAb labeling of necrotic cells was observed without detergent permeabilization.

than live cells (compare Figures 4 and 6). Cyt *c*-specific mAb labeling of the heat-shocked cells was similar to the labeling of the R2 population of post-apoptotic cells, i.e., without permeabilization and/or fixation (Figure 6). Thus, the level of binding of the native cyt *c*-specific mAb 2G8.B9 was decreased relative to the level of binding of 2.7D5, and there was a concomitant increase in the level of binding of mAb 1D3 which recognizes a non-native form of cyt *c*.

The confocal micrographs in Figure 5 (right panels) show the staining pattern of cyt *c* in necrotic DO11.10 cells. The labeling by either mAb 2.7D5 or mAb 1D3 was diffuse and polarized to one end of the cell with a lack of punctate staining, clearly different than the patterns observed in live or apoptotic cells.

Antibodies That Are Reactive Only with Short Peptides Did Not Label Cyt c of Live, Apoptotic, or Necrotic Cells. Polyclonal rabbit antibodies that were reactive with short peptides of cyt *c* corresponding to the amino terminus (residues 1−4) or middle of the polypeptide chain (residues 41−48) and a mouse mAb (7H8) that was reactive with the carboxyl terminus (residues 93−104) did not label either live DO11.10 cells, the R1′ or R2 subpopulations of pre-apoptotic and post-apoptotic DO11.10 cells, or the R3 populaton of necrotic cells (results not shown). Also, polyclonal mouse antibodies elicited against the 1−80 fragment of horse cyt *c*

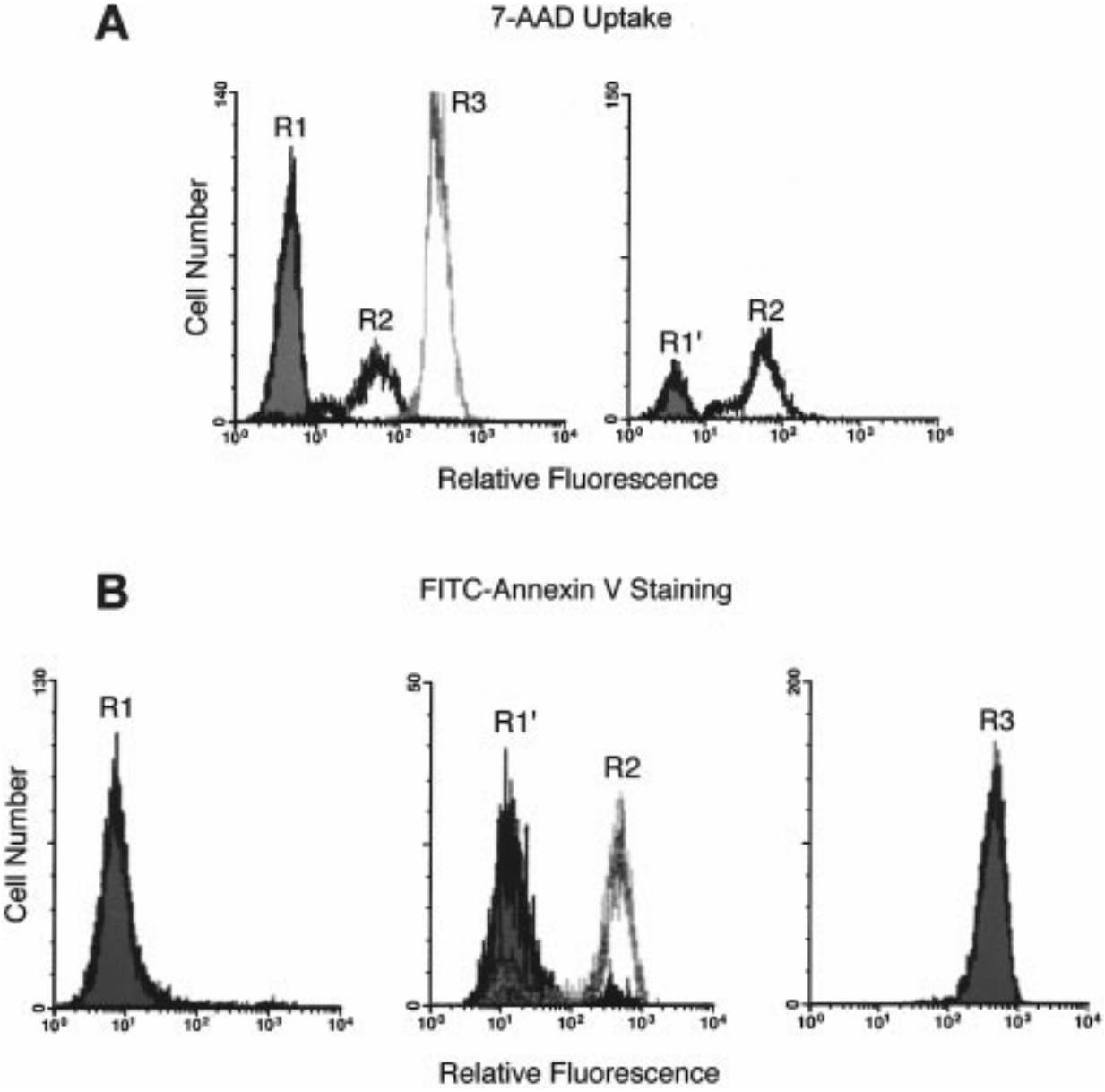

FIGURE 7: Identification of live, apoptotic, and necrotic subpopulations of DO11.10 cells based on their uptake of 7-AAD (top panel) and staining with FITC-annexin V (bottom panel). The R1′ subpopulation of DO11.10 cells, like the viable cells, remains impermeable to 7-AAD and is weakly stained with FITC-annexin V. Therefore, R′ cells appear to be pre-apoptotic even though a change in the conformation of intracellular cyt *c* is already apparent (see Figure 4).

did not label cyt *c* in these cells. All of the peptide-reactive antibodies recognize denatured cyt *c* as shown by their binding to cyt *c* adsorbed to microtiter plates in indirect ELISAs (results not shown). In addition, the antibodies that were reactive with residues 93−104 and 1−80 have been shown to bind apocyt *c* (obtained from *Drosophila* as an [^{35}S]methionine-labeled product and tested for antibody binding by immunoprecipitation; R. Jemmerson and E. Margoliash, unpublished results). Thus, the failure of the peptide-reactive antibodies to recognize cyt *c* in either live or dead cells indicates that neither apocyt *c* nor (grossly) denatured forms of cyt *c* can be detected in the cells.

Distinction among the Subpopulations of DO11.10 Cells Based on Uptake of 7-AAD and Staining with FITC-Annexin V. The fluorescent dye 7-AAD which binds DNA is a marker for apoptosis (*33*). Its staining pattern confirmed the distinctions among the various cell subpopulations based on FSC versus SSC. The post-apoptotic R2 subpopulation of DO11.10 cells absorbed significantly more dye than did the R1 cells (Figure 7A, left panel). The heat-shocked (R3) DO11.10 cells absorbed even more dye than the post-apoptotic cells. R1′ cells, the other subpopulation in the apoptotic mixture of DO11.10 cells, were similar to the R1 cells in that they failed to absorb 7-AAD (Figure 7A, right panel). Similar results were obtained when the cells were stained with FITC-annexin V which detects phosphatidylserine displaced from the cytoplasmic surface of the cell membrane to the outside surface (*34*). Live cells (R1) could not be stained with FITC-annexin V (Figure 7B, left panel). In necrosis, cells become permeable to annexin V so the cytoplasmic face of the membrane is heavily labeled (Figure 7B, right panel). R2, post-apoptotic, cells showed an intermediate level of staining (Figure 7B, middle panel). The R1′ subpopulation of apoptotic cells showed perhaps slight staining since the

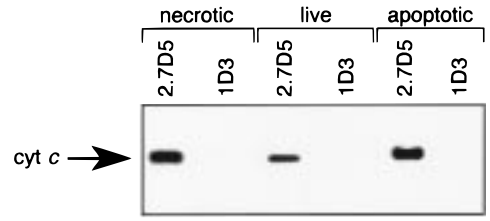

FIGURE 8: Western blot of cyt *c* immunoprecipitated from live, apoptotic, and necrotic DO11.10 cells. Following indirect immunoprecipitation of cyt *c* using protein G−agarose, precipitated proteins were boiled in sodium dodecyl sulfate, electrophoresed in SDS−PAGE, electroblotted onto nitrocellulose, and probed with mAb 7H8 (7H8.2C12) which is specific for denatured cyt *c*. Cyt *c* was indirectly visualized using horseradish peroxidase conjugated to goat anti-mouse IgG. mAb 2.7D5 immunoprecipitated cyt *c* extracted with detergent from each cell type. mAb 1D3 did not immunoprecipitate soluble cyt *c* extracted from any of the cells.

relative fluorescence was shifted to the right compared to that of the R1 population. This is consistent with the interpretation that the R1′ cells represent an early apoptotic or pre-apoptotic subpopulation.

Immunoprecipitation of Cyt c Extracted from Live, Apoptotic, and Necrotic DO11.10 Cells. To examine whether the conformational change in cyt *c* that could be detected in apoptotic and necrotic cells by mAb 1D3 binding was due to a covalent modification of cyt *c*, proteins were extracted from DO11.10 cells in detergent, immunoprecipitated with mAbs to cyt *c*, and examined in Western blots using a mAb (7H8) specific for the carboxyl terminus of cyt *c*. While mAb 2.7D5 recognized cyt *c* extracted from live, apoptotic, and necrotic cells, mAb 1D3 did not recognize cyt *c* in the same extracts (Figure 8).

The Heavy Membrane Fraction of Post-Apoptotic Cells Is Functional in Caspase Activation. The immunofluorescent confocal microscopy results suggested that cyt *c* remained bound to mitochondria in post-apoptotic cells. To examine whether the mitochondria-associated cyt *c* was functional in caspase activation, we tested the heavy membrane (mitochondria-containing) fractions of live and post-apoptotic cells for PARP cleavage in the presence of the S-100 fraction (cytosol) of live cells. A constitutive cytosolic protein, Apaf-1, in conjunction with dATP and cyt *c* as a cofactor has been shown to cleave pro-caspase 9 to its active form which, in turn, cleaves pro-caspase 3 (*35*). Activated caspase 3 cleaves PARP. Therefore, PARP cleavage is an indirect indicator of the pro-apoptotic function of cyt *c*. Nevertheless, cyt *c* is the only known mitochondrial cofactor for caspase activation so that a requirement for mitochondria in caspase activation would implicate cyt *c*.

Results of a Western blot for observing PARP cleavage are shown in Figure 9. The heavy membrane fraction of post-apoptotic cells in conjunction with the S-100 fraction of live cells was functional in caspase activation. The intensity of the band for cleaved PARP varied directly with the volume of the heavy membrane fraction added (not shown). Neither the heavy membrane fraction of live cells nor the supernatant from the last wash of post-apoptotic mitochondria was functional. This suggests that a change in the disposition or context of cyt *c* in mitochondria of apoptotic cells rather than its release into the cytosol allows it to serve as a cofactor in caspase activation in the T hybridoma cells.

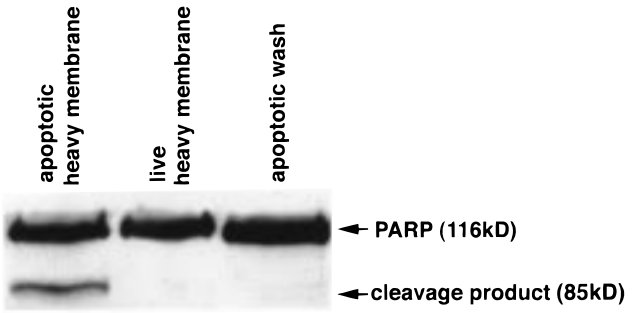

FIGURE 9: Western blot of PARP demonstrating that the heavy membrane fraction containing mitochondria of post-apoptotic cells retains a cofactor for caspase activation. The heavy membrane fractions of live and post-apoptotic cells or the final wash of the apoptotic membranes were incubated with the S-100 fraction of live cells along with PARP and dATP. The extent of cleavage of PARP is an indirect indicator of the function of cyt *c* as a cofactor in the activation of caspase 9.

DISCUSSION

Cyt *c* plays important roles in both the life and death of a cell. In life, cyt *c* is involved in respiration, transferring electrons to cytochrome oxidase for reduction of oxygen (*36*). In programmed cell death or apoptosis, translocation of cyt *c* from its normal location between the inner and outer mitochondrial membrane has been reported to allow cyt *c* to serve as a coactivator of the enzyme caspase 9 (*14*, *37*), an initiator off the apoptotic pathway. Although much is known about the structure and function of cyt *c* in vitro, how it functions as a coactivator in apoptosis is not known, and the physiological context of cyt *c* in the life and death processes in which it plays a role is poorly defined.

An approach for studying the context of cyt *c* in the respiratory chain has been to examine the interaction of cyt *c* not only with its partners in electron transport (*38*−*42*) but also with model membranes, e.g., synthetic phospholipid membranes to represent the phospholipid-rich inner mitochondrial membrane (*1*−*7*). From such studies in which biophysical methods were employed, convincing evidence has been obtained supporting the idea that cyt *c* undergoes a conformational change when bound to phospholipids (*1*−*6*). Therefore, it has been inferred by some that cyt *c* can interact not only with its electron exchange partners but also with the inner mitochondrial membrane and, in the latter case, undergoes a conformational change.

Using a mAb that is reactive with a defined region of a native-like form of cyt *c*, we have confirmed a change in the conformation of the cyt *c* polypeptide when it binds to synthetic phospholipid vesicles. This mAb also detected a conformational change in the alkaline isomer of cyt *c*, consistent with previous biophysical studies which indicated similarities between phospholipid-bound and alkaline cyts *c* (*1*−*6*, *31*). The conformational change detected with mAb 1D3 involves the region around residue 44 which is part of an omega loop in native cyt *c* and is located to the right and below the exposed heme crevice (*15*). A change in the conformation of this region is consistent with the results of previous studies which showed a loss of one of the ligands of the polypeptide to the heme and loss of H-bonds between certain amino acid side chains and one of the heme propionates when cyt *c* associates with phospholipids (*1*−*6*). The conformational change in cyt *c* of dead cells may

be localized to the heme crevice and nearby areas. In this study, mAb 2.7D5, which is reactive with the region around residue 62 on native cyt *c*, recognized cyt *c* in both live and dead cells. Furthermore, none of the short peptide-reactive mAbs recognized cyt *c* in dead cells, arguing against a global disruption in the conformation or proteolysis of the protein. The conformational change detected by mAb 1D3 is not simply due to a change in the oxidation state of cyt *c*. In a competitive ELISA, cyt *c* oxidized with potassium ferricyanide or reduced with sodium dithionite did not bind mAb 1D3 (results not shown). Furthermore, the binding of mAb 1D3 to cyt *c* in necrotic (heat-shocked) cells is not due to thermal denaturation. When purified cyt *c* was preheated to 65 °C for 5 min, it did not bind mAb 1D3 in a competitive ELISA (results not shown).

Indirect immunofluorescent labeling of the T cell hybridoma, DO11.10, by mAb 1D3 and mAb that was reactive with native cyt *c* indicates that the conformational change which occurs in cyt *c* bound to phospholipid vesicles cannot be detected in live cells. This suggests that it may not be relevant to the function of cyt *c* as an electron transport protein, at least in the transformed cells that we studied. However, in cell death, whether by apoptosis or necrosis, this conformational change can be detected. This change is not peculiar to the means in which cell death was initiated or to this particular cell type. In this study, similar patterns of mAb binding were observed whether DO11.10 cells were induced to apoptose by dexamethasone or were heat shocked. Comparable results were obtained when the DO11.10 cells were induced to apoptose by activation with an immobilized anti-T cell receptor (CD3) mAb or by γ-irradiation (results not shown). A similar analysis of HeLa (human adenocarcinoma) cells induced to apoptose by staurosporine treatment also showed binding by mAb 1D3 and mAb 2.7D5 without permeabilizing the cells (results not shown).

To be rigorous, we should consider the possibility that in the context of a cell, mAb 1D3 may not react with cyt *c* but with some unrelated epitope that is, coincidentally, exposed only in dead cells. The most compelling argument against this possibility is that as the binding of mAb 1D3 became apparent in dead cells there was a concomitant decrease in the level of binding of mAb 2G8.B9 which recognizes the same region of cyt *c* around residue 44 but only on native cyt *c*. Consistent with the punctate labeling of mAb 1D3, we have shown that caspase coactivation, attributed to cyt *c*, is retained in the mitochondrial-containing fraction of post-apoptotic T hybridoma cells. Similarly, in a human T cell line, a loss in the functional activity of cyt *c* has been shown to occur early in apoptosis (*43*) without the apparent efflux of cyt *c* from mitochondria (*43*, *44*). Finally, in a study of *Drosophila* nurse cells undergoing apoptosis during oogenesis, "unmasking" of an epitope in *Drosophila* cyt *c*, identified by an mAb different than 1D3, has been observed early in apoptosis (*45*). In that case, it has not been shown that the unmasking of the epitope is due to a conformational change.

Since mAb 1D3 detects cyt *c* bound to synthetic phospholipid vesicles, cyt *c* may undergo a conformational change in apoptotic and necrotic cells when it associates with membranes altered during the death process. Alterations in the plasma membrane are known to occur during cell death, e.g., redistribution of phosphatidylserine from the inner leaflet to the outer leaflet (*34*). Therefore, changes in other membranes in dying cells would seem likely. The distribution of phospholipids, by affecting negative charge density, does influence the binding of cyt *c* to synthetic vesicles (*46*) and could explain the phenomenon described here.

The fact that mAb 1D3 does not immunoprecipitate cyt *c* extracted from dead cells with detergent is consistent with the idea that this conformational change is not due to a covalent modification in cyt *c*. It may be due to association of cyt *c* with some other cellular component. In apoptosis cyt *c*, also known as Apaf-2, binds to another pro-apoptotic factor, Apaf-1. While we have been able to immunoprecipitate the complex of cyt *c* and Apaf-1 with mAb 2.7D5, it has not been immunoprecipitated with mAb 1D3 (J. Liu and R. Jemmerson, unpublished), indicating that the conformational change in cyt *c* detected by mAb 1D3 is not due to its association with Apaf-1. However, Apaf-1 may still recognize conformationally altered cyt *c* that appears to remain associated with mitochondria in apoptotic cells. Indeed, using the extent of PARP cleavage as a readout, the heavy membrane fraction of post-apoptotic cells was able to facilitate caspase activation. This is consistent with results of a study in *Drosophila* in which the heavy membrane fraction containing cyt *c* was also shown to function as a cofactor in caspase activation (*45*). It should be noted that contradictory evidence has been obtained in a number of studies which shows that cyt *c* effluxes from mitochondria during apoptosis (*14*, *47*−*50*). This controversy may be resolved by noting differences in the cell types examined and/or differences in the conditions under which the cells were extracted and fractionated. For example, ionic strength is known to affect the association of cyt *c* with synthetic membranes (*51*).

The conformational change in cyt *c* of dying cells may be relevant to the recognition of endogenous cyt *c* by B lymphocytes. If membrane-associated cyt *c* is a form of the self-antigen that is "seen" by developing B cells, then the altered conformation around residue 44 may lead to tolerance in B cells that recognize it. This may explain the significantly reduced frequency of B cells in mouse spleen versus bone marrow that are specific for the 41−49 peptide of mouse cyt *c* (*52*). Since the mAbs produced by these B cells do not recognize native cyt *c*, it is not understood how the apparent tolerance of those B cells was acquired. The conformational change could also affect how cyt *c* is recognized by the immune system in some types of autoimmunity (*16*).

ACKNOWLEDGMENT

We are grateful to Dr. Emanuel Margoliash for providing some of the cyts *c* used in this study, Dr. Xiaodong Wang for recombinant Apaf-1, Dr. Patrick Schlievert for a control mAb, and Dr. John Abrams for helpful discussions.

REFERENCES

1. Hildebrandt, P., Heimburg, T., and Marsh, D. (1990) *Eur. Biophys. J. 18*, 193−201.
2. Spooner, P. J. R., and Watts, A. (1991) *Biochemistry 30*, 3880−3885.
3. Spooner, P. J. R., and Watts, A. (1992) *Biochemistry 31*, 10129−10138.
4. Heimburg, T., Hildebrandt, P., and Marsh, D. (1991) *Biochemistry 30*, 9084−9089.

5. Soussi, B., Bylund-Fellenius, A.-C., Scherstén, T., and Ångström, J. (1990) *Biochem. J. 265*, 227−232.
6. Muga, A., Mantsch, H. H., and Surewicz, W. K. (1991) *Biochemistry 30*, 7219−7224.
7. Salamon, Z., and Tollin, G. (1996) *Biophys. J. 71*, 848−857.
8. Sela, M., Schechter, B., Schechter, I., and Borek, F. (1967) *Cold Spring Harbor Symp. Quant. Biol. 32*, 537−545.
9. Sachs, D. H., Schechter, A. N., Eastlake, A., and Anfinsen, C. B. (1972) *Proc. Natl. Acad. Sci. U.S.A. 69*, 3790−3794.
10. Goshorn, S. C., Retzel, E., and Jemmerson, R. (1991) *J. Biol. Chem. 266*, 2134−2142.
11. Minnerath, J. M., Mueller, C. M., Buron, S., and Jemmerson, R. (1995) *Eur. J. Immunol. 25*, 784−791.
12. Mueller, C. M., and Jemmerson, R. (1996) *J. Immunol. 157*, 5329−5338.
13. Shimonkevitz, R., Colon, S., Kappler, J. W., Marrack, P., and Grey, H. (1984) *J. Immunol. 133*, 2067−2074.
14. Liu, X., Kim, C. N., Yang, J., Jemmerson, R., and Wang, X. (1996) *Cell 86*, 147−157.
15. Bushnell, G. W., Louie, G. V., and Brayer, G. D. (1990) *J. Mol. Biol. 214*, 585−595.
16. Mamula, M. J., Jemmerson, R., and Hardin, J. A. (1990) *J. Immunol. 144*, 1835−1840.
17. Borden, D., and Margoliash, E. (1975) in *Handbook of Biochemistry and Molecular Biology, Proteins* (Fasman, G. D., Ed.) Vol. III, pp 155−182, The Chemical Rubber Co., Cleveland, OH.
18. Corradin, G., and Harbury, H. A. (1970) *Biochim. Biophys. Acta 221*, 489−496.
19. Jemmerson, R., and Hutchinson, R. M. (1990) *Eur. J. Immunol. 20*, 579−585.
20. Urbanski, G. J., and Margoliash, E. (1977) *J. Immunol. 118*, 1170−1180.
21. Jemmerson, R., and Johnson, J. G. (1991) *Proc. Natl. Acad. Sci. U.S.A. 88*, 4428−4432.
22. Rytömaa, M. (1996) Molecular Mechanisms of Interactions Between Cytochrome c and Acidic Phospholipids, Ph.D. Dissertation, University of Helsinki, Helsinki, Finland.
23. Jemmerson, R., Johnson, J. G., Burrell, E., Taylor, P. S., and Jenkins, M. K. (1991) *Eur. J. Immunol. 21*, 143−151.
24. Zacharchuk, C. M., Mercep, M., Chakraborti, P. K., Simons, S. S., Jr., and Ashwell, J. D. (1990) *J. Immunol. 145*, 4037−4045.
25. Leo, O., Foo, M., Sachs, D. H., Samelson, L. E., and Bluestone, J. A. (1987) *Proc. Natl. Acad. Sci. U.S.A. 84*, 1374−1378.
26. Millan, J. L., and Stigbrand, T. (1983) *Eur. J. Biochem. 136*, 1−7.
27. Brelje, T. C., Wessendorf, M. W., and Sorenson, R. L. (1993) *Methods Cell Biol. 28*, 97−181.
28. Minnerath, J. M., Crump, B. L., Margoliash, E., and Jemmerson, R. (1995) *Mol. Immunol. 32*, 795−803.
29. Jemmerson, R. (1995) in *Immunological Recognition of Peptides in Medicine and Biology* (Zegers, N. D., Boersma, W. J. A., and Claassen, E., Eds.) pp 213−225, CRC Press, Boca Raton, FL.
30. Nicholls, P., and Malviya, A. N. (1973) *Biochem. Soc. Trans. 1*, 372−375.
31. Smith, H. T., and Millett, F. (1980) *Biochemistry 19*, 1117−1120.
32. Casciola-Rosen, L. A., Anhalt, G., and Rosen, A. (1994) *J. Exp. Med. 179*, 1317−1330.
33. Schmid, I., Uittenbogaart, C. H., Keld, B., and Giorgi, J. V. (1994) *J. Immunol. Methods 170*, 145−157.
34. Vermes, I., Haanen, C., Steffens-Nakken, H., and Reutelingsperger, A. C. (1995) *J. Immunol. Methods 184*, 39−51.
35. Li, P., Nijhawan, D., Budihardjo, I., Srinivasula, S. M., Ahmad, M., Alnemri, E. S., and Wang, X. (1997) *Cell 91*, 479−489.
36. Pettigrew, G. W., and Moore, G. R. (1987) *Cytochromes c-biological aspects*, Springer-Verlag, Berlin, Heidelberg, New York, London, Paris, and Tokyo.
37. Li, P., Nijhawan, D., Budihardjo, I., Srinivasula, S. M., Ahmad, M., Alnemri, E. S., and Wang, X. (1997) *Cell 91*, 470−489.
38. Staudenmayer, N., Ng, S., Smith, M. B., and Millett, F. (1977) *Biochemistry 16*, 600−604.
39. Ng, S., Smith, M. B., Smith, H. T., and Millett, F. (1977) *Biochemistry 16*, 4975−4978.
40. Ferguson-Miller, S., Brautigan, D. L., and Margoliash, E. (1978) *J. Biol. Chem. 253*, 149−159.
41. Speck, S. H., Ferguson-Miller, S., Osheroff, N., and Margoliash, E. (1979) *Proc. Natl. Acad. Sci. U.S.A. 76*, 155−159.
42. Salamon, Z., and Tollin, G. (1996) *Biophys. J. 71*, 858−867.
43. Krippner, A., Matsuno-Yagi, A., Gottlieb, R. A., and Babior, B. M. (1996) *J. Biol. Chem. 271*, 21629−21636.
44. Adachi, S., Cross, A. R., Babior, B. M., and Gottlieb, R. A. (1997) *J. Biol. Chem. 272*, 21878−21882.
45. Varkey, J., Chen, P., Jemmerson, R., and Abrams, J. M. (1999) *J. Cell Biol.* (in press).
46. Mustonen, P., Virtanen, J. A., Somerharju, P. J., and Kinnunen, P. K. J. (1987) *Biochemistry 26*, 2991−2997.
47. Yang, J., Liu, X., Bhalla, K., Kim, C. N., Ibrado, A. M., Cai, J., Peng, T.-I., Jones, D. P., and Wang, X. (1997) *Science 275*, 1129−1132.
48. Kluck, R. M., Bossy-Wetzel, E., Green, D. R., and Newmeyer, D. D. (1997) *Science 275*, 1132−1136.
49. Rossé, T., Olivier, R., Monney, L., Rager, M., Conus, S., Fellay, I., Jansen, B., and Borner, C. (1998) *Nature 391*, 496−499.
50. Jürgensmeier, J. M., Xie, Z., Deveraux, Q., Ellerby, L., Bredesen, D., and Reed, J. C. (1998) *Proc. Natl. Acad. Sci. U.S.A. 95*, 4997−5002.
51. Heimburg, T., and Marsh, D. (1995) *Biophys. J. 68*, 536−546.
52. Klinman, N. R., Riley, R. L., Morrow, P. R., Jemmerson, R. R., and Teale, J. M. (1985) *Fed. Proc. 44*, 2488−2492.

BI9809268